AD-A222 827

1. AG...	y 1990	3. REPORT TYPE AND DATES COVERED: Journal Article

4. TITLE AND SUBTITLE
Polar Coordinate Laser Writer for Binary Optics Fabrication

5. FUNDING NUMBERS
C-F19628-90-C-0002

PE-600

6. AUTHOR(S)
Goltsos, William L. Dr., Liu, Sharlene

7. PERFORMING ORGANIZATION NAME(S) AND ADDRESS(ES)
Lincoln Laboratory, M.I.T.
P.O. Box 73
Lexington, MA. 02173

8. PERFORMING ORGANIZATION REPORT NUMBER
MS-8737

9. SPONSORING/MONITORING AGENCY NAME(S) AND ADDRESS(ES)
Defense Research Projects Agency
1400 Wilson Blvd.
Arlington, Virginia, 22209

10. SPONSORING/MONITORING AGENCY REPORT NUMBER
ESD-TR- 90-061

11. SUPPLEMENTARY NOTES
SPIE Vol. 1211 Computer & Optically FOrmed Holographic Optics (1990)

12a. DISTRIBUTION/AVAILABILITY STATEMENT
Approved for public Release: Distribution unlimited

12b. DISTRIBUTION CODE

13. ABSTRACT *(Maximum 200 words)*

A Laser Writer system for recording centro-symmetric patterns in photoresist has been developed as an alternative method for binary optics mask and component fabrication.This system is capable of generating binary amplitude patterns with linewidths below 1 μm and with a positional accuracy of less than 0.1μm on up to 3 in. diameter planar substrates. The measured wavefront error and diffraction efficiency of a direct-write two-phase-level F/10 lens confirm that high quality components can be fabricated quickly, easily, and at low cost.

14. SUBJECT TERMS
Bibary Optics Fabrication, Polar Coordinate Laser
Centro-symmetric patterns

15. NUMBER OF PAGES
12

16. PRICE CODE

17. SECURITY CLASSIFICATION OF REPORT	18. SECURITY CLASSIFICATION OF THIS PAGE	19. SECURITY CLASSIFICATION OF ABSTRACT	20. LIMITATION OF ABSTRACT
Uncl.	Uncl.	Uncl.	

PROCEEDINGS REPRINT

SPIE—The International Society for Optical Engineering

Reprinted from

Computer and Optically Formed Holographic Optics

15–16 January 1990
Los Angeles, California

Volume 1211

Polar Coordinate Laser Writer for Binary Optics Fabrication

William Goltsos and Sharlene Liu*

Lincoln Laboratory,Massachusetts Institute of Technology
244 Wood Street, Lexington, Massachusetts 02173

ABSTRACT

A Laser Writer system for recording centro-symmetric patterns in photoresist has been developed as an alternative method for binary optics mask and component fabrication.This system is capable of generating binary amplitude patterns with linewidths below 1 μm and with a positional accuracy of less than 0.1μm on up to 3 in. diameter planar substrates. The measured wavefront error and diffraction efficiency of a direct-write two-phase-level F/10 lens confirm that high quality components can be fabricated quickly, easily, and at low cost.

1. INTRODUCTION

Binary optics has been successfully applied in such areas as coherent beam addition[1], refractive optics aberration corrections[2] and agile beam steering[3]. The capability offered by this diffractive optics technology, to implement nearly arbitrary phase profiles and aperture shapes, remains difficult to achieve using conventional optical techniques.

Binary optics utilizes high-resolution lithography and ion-beam etching techniques to create binary or multi-level surface relief patterns in dielectric or metallic substrates. The surface profile of a properly etched diffractive optical element forms a stair-case approximation to a desired continuous phase contour evaluated modulo 2π.[4] In general, the diffraction efficiency of an optical element increases with the number of quantized phase levels in the step-wise approximation.

Masks, used during component fabrication to define the etched areas of a substrate surface, are commonly recorded with an electron beam (E-beam) pattern generator. The high accuracy of an E-beam machine is essential in many applications since mask quality has a significant impact on optical element performance. While E-beam pattern generators offer very high precision and demonstrate excellent flexibility in terms of pattern geometries, such machines require large data files to specify even very simple patterns. For example, although just two parameters–inner and outer radii–uniquely define a radially symmetric feature, over 1000 parameters are needed to describe this same feature in an E-beam compatible format. Therefore, at least for the centro-symmetric subset of binary optics patterns, writing the data files required for an E-beam pattern generator adds unnecessary computational complexity, time, and cost to the mask fabrication process.

In this paper we propose a laser writer mask fabrication tool that intrinsically writes radially symmetric patterns, especially patterns for spherical and chromatic aberration correction of hybrid diffractive/refractive optics. While such machines have been described in the literature for recording patterns having either radial[5] or arbitrary symmetry[6,7], the importance of an alternative to E-beam mask fabrication for the rapid assimilation of binary optics into tomorrows optics industry suggests the need to develop a tool which is fast, easy to use and inexpensive to operate. By exclusively utilizing mature technologies, the machine presented here fulfills these requirements and has the additional benefits of low development time, low cost, and high operational reliability.

*Present address:Department of Electrical Engineering and Computer Science, Massachusetts Institute of Technology, Cambridge, Ma. 02139

2. LASER WRITER COMPONENTS

The laser writer system described here resembles, both in principle and practice, a diamond turning machine where the diamond cutting tool is replaced with a laser beam for exposing photoresist. A schematic diagram of our polar-coordinate laser writer is shown in Fig. 1. Whenever possible, off-the-shelf components were employed in the construction of our system to reduce development time and cost.

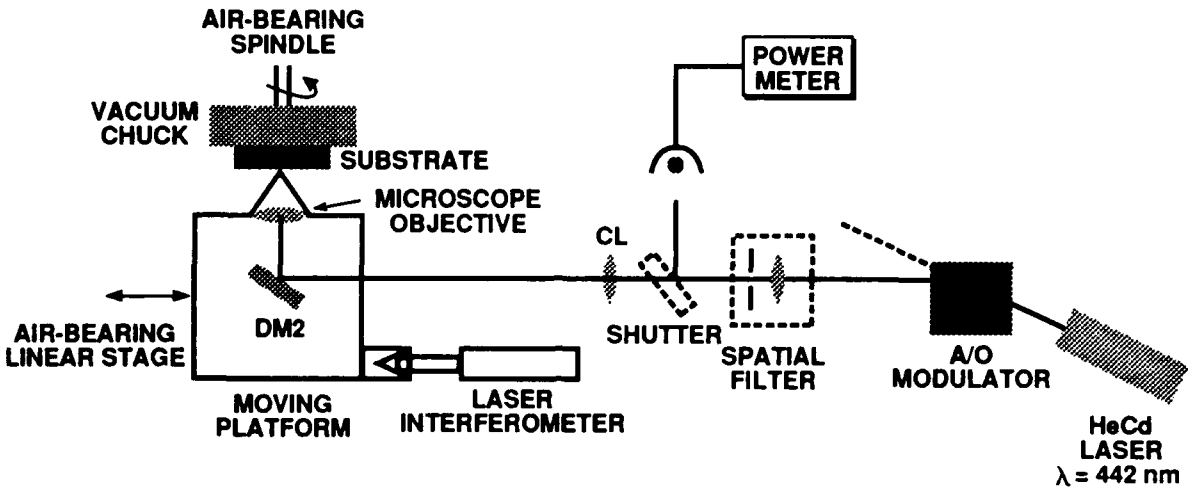

Figure 1: Schematic diagram of the polar-coordinate laser writer system. DM=dichroic mirror.

2.1. Mechanics

A photoresist-coated substrate is mounted in the vacuum chuck of a high precision air-bearing spindle. The spindle shaft is driven by a brushless DC motor and its angular position and velocity are measured by an optical encoder. The angular velocity is servo-controlled to within 0.3% of a 60-1000 RPM set point. Spindle radial runout, specified to be less than 0.02 μm, accounts for 20% of the entire laser writer system positioning error.

The spindle and a linear air-bearing slide are mounted on a granite slab with the spindle rotation axis and slide translation axis orthogonally oriented . The linear slide carries the traveling platform optics, and therefore establishes the write beam radial position on the substrate. Since the overall system performance depends largely on the accuracy of this slide, a double-pass laser-interferometer ($\lambda/16 = 0.04\ \mu m$ resolution) is used to servo-control its position through a stepper-motor-driven lead-screw. A factor that affects pattern write times, and will be discussed later, is the slide settling time. After slide translation at 1.3 mm/s, the slide settles to within 0.1 μm about its final position in less than 0.5 s. Figure 2 is a photograph of the air-bearing components and traveling platform optics.

2.2. Optics

Linearly polarized light from the 14 mW He-Cd laser source ($\lambda = .442\mu m$) is diffracted by an acousto-optic (A-O) modulator and passed through the pinhole of a spatial filter. This configuration results in 30 dB of analog intensity modulation where the beam alignment after the pinhole is maintained despite laser pointing instabilities and thermal effects in the modulator crystal. A beam steering shutter is located after the spatial filter to direct the modulated light beam onto a power

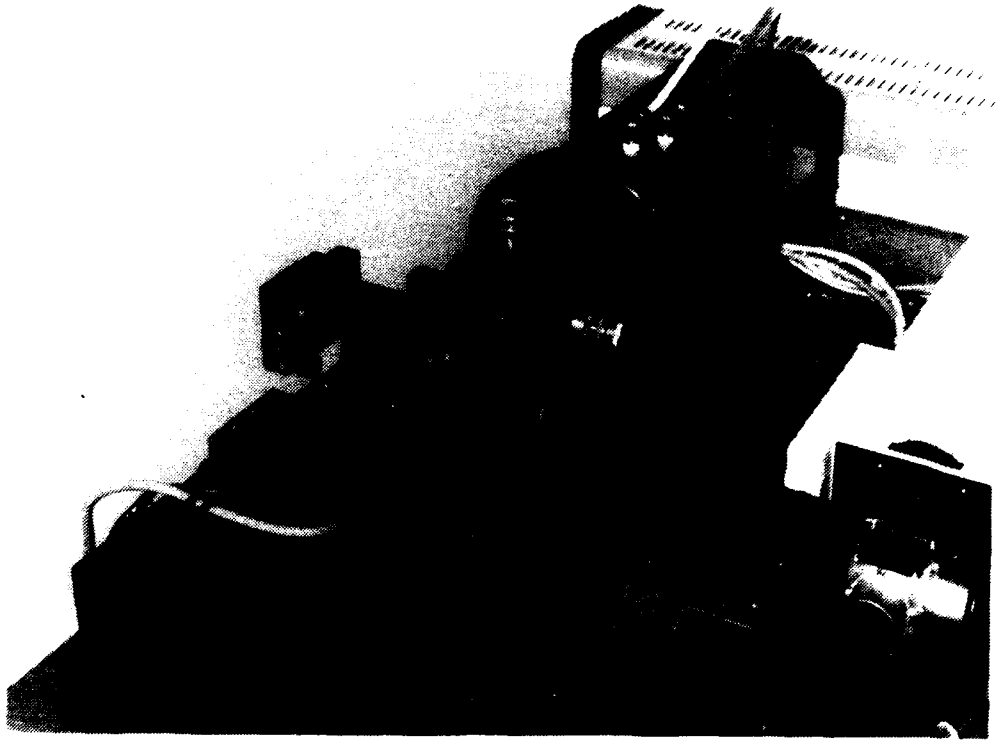

Figure 2: Photograph of the laser writer air-bearing slide and spindle, and moving platform optics. The helium-cadmium laser source is visible in the background and the laser interferometer, for controlling the slide position, is in the right foreground.

monitor whenever photoresist exposure is not desired. Following recollimation, the conditioned beam propagates parallel to the slide translation axis and is directed through a 0.55 numerical aperture microscope objective by a 75% reflecting dichroic mirror (DM2 in Fig. 1), focusing on the substrate surface.

Two additional key functions are performed by the dichroic mirrors (DM1 and DM2 in Fig. 3) mounted on the traveling platform. First, these dichroic mirrors allow the infrared autofocus beam to propagate collinearly with the write beam through the focusing microscope objective (MO). This autofocus system is described in more detail below. Second, the dichroic mirror (DM2), together with the reflecting surface of the rotating substrate and the mirror (M) form a Michelson interferometer whose output is magnified by the lens (L) and projected onto a screen. While this interferometer can be used to monitor visually the write beam focus condition during write time by noting curvature of the interference fringes, its main purpose is to locate the spindle rotation axis prior to write time.

The spindle rotation axis, which defines the origin of the polar coordinate system, is found by mounting a wedged reflecting substrate in the vacuum chuck. With the write beam focused onto the wedged substrate, any surface axial runout due to a spatial offset of the write beam focal spot from the rotation axis will cause a variation in the interference pattern. This fringe modulation is syncronized with the spindle rotation and can be minimized by translating the microscope objective in a plane normal to the rotation axis. Decentration errors of less than 0.2 μm can be readily achieved by this technique with a 10° wedged substrate.

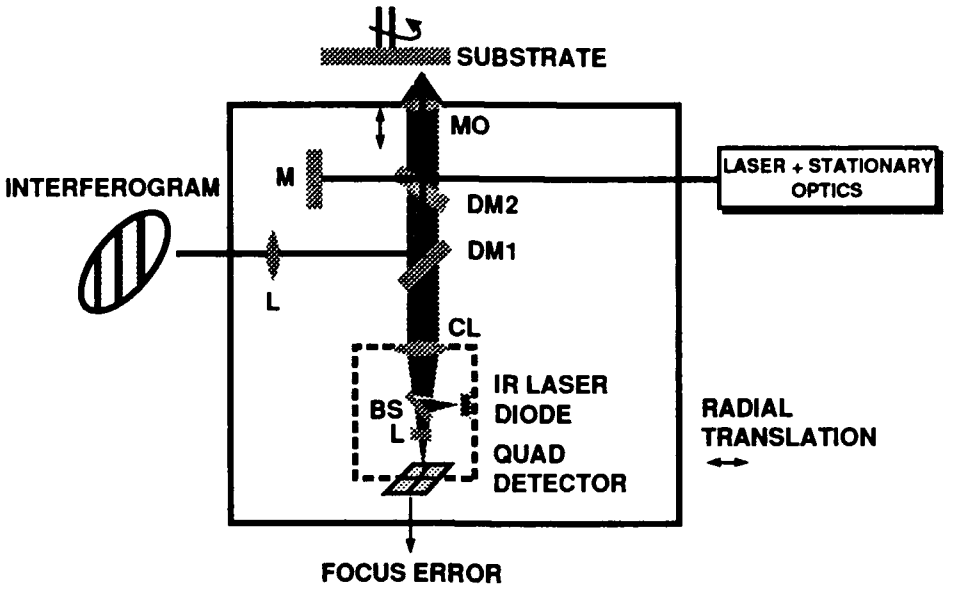

Figure 3: Schematic diagram of the moving platform optics. MO=microscope objective, M=mirror, DM=dichroic mirror, L=lens, CL=collimating lens, and BS=beam splitter.

2.3. Auto-focus system

The major contributors to substrate surface axial runout are substrate wedge and nonuniform contact between the substrate and spindle face. To counteract these defocusing effects an autofocus system is incorporated into the traveling optical system. The microscope objective is mounted in a three-axis positioner such that two axes can be used for locating the spindle rotation axis, as descibed above. The third axis provides a focus adjustment of the microscope objective and is actuated by a piezo-electric translator. Focus error is converted into an electrical signal by an astigmatic lens transducer [8] that was obtained from a compact disk player. A dedicated computer monitors focus error and generates a correction signal to drive the focus translator.

The focus correction signal generated by the computer has two components. The first component is a sinusoid syncronized with the spindle rotation for compensating the defocusing effects described above. The amplitude of this sinusoid is servo-controlled and is dependent on the write beam radial position. The second component is a dc bias that neutralizes any initial focus offset, and therefore eliminates the need to accurately focus the beam by a manual adjustment. Focus errors of less then 0.1 μm are readily detected with this autofocus system and rarely exceed ± 0.2 μm during write time. This is well within the ± 0.6 μm depth-of-focus of the microscope objective.

2.4. Process control

Write-time processes are coordinated by an 80386/80387-based personal computer (PC). Both before a pattern is written and periodically during write time, the PC interogates a barometric pressure transducer and compensates the air-bearing slide radial position for interferometer optical path length variations caused by local changes in the refractive index of air (n_a). Given barometric pressure, temperature and relative humidity, n_a is calculated from an analytic approximation.[9] The computer also corrects the write beam intensity (to better than 1%) before writing each zone on the substrate in order to maintain optimum photoresist exposure conditions. The beam intensity is

increased linearly with slide radial position to compensate for the decrease in effective exposure time that results from a constant spindle angular velocity. This process also minimizes undesirable beam intensity variations caused by laser power fluctuations, laser pointing instabilities and beam steering effects due to temperature fluctuations in the A-O modulator. Exposure duration is syncronized by the PC with spindle rotation and slide motion,as outlined below. Commands for stage motion are derived from a data file that is stored on the PC hard disk prior to write time. A simplified block diagram of the process control system is shown in Fig. 4.

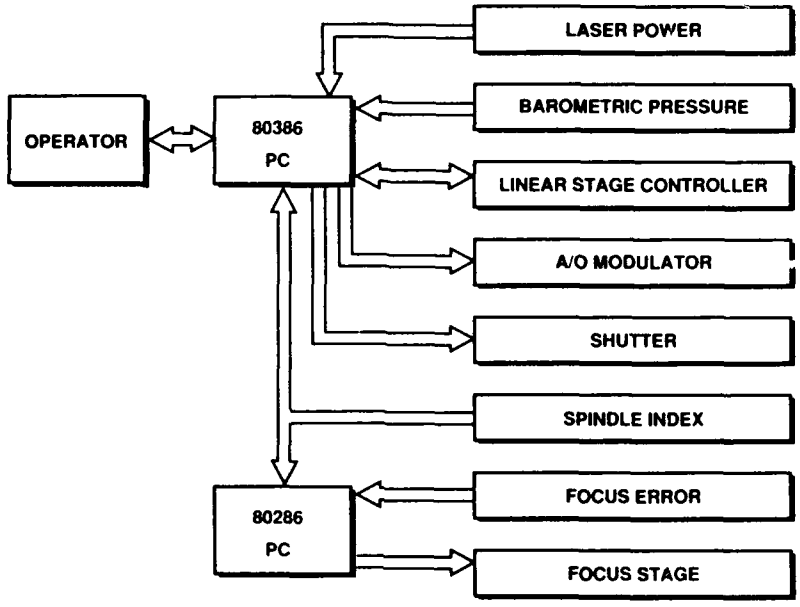

Figure 4: Block diagram of the laser-writer process control system. Arrows indicate the direction of communication.

2.5. Environmental control

The laser writer mechanical and optical components are mounted on a pneumatically isolated table and enclosed by an environmental chamber to insure the alignment and length stability of critical components that may be affected by building vibrations and temperature fluctuations. The environmental chamber (custom manufactured by Semifab Inc.,Hollister,Ca.), shown in Fig. 5, is designed to maintain a specific temperature and relative humidity to within ± 0.1 degrees C and $\pm 4.0\%$, respectively. Humidity and temperature are controlled to minimize interferometer optical path length variations caused by local changes in n_a. The recirculating air is filtered to Class 100 standards and flows vertically over the laser writer components at speeds up to 75 linear feet per minute.

3. WRITING FORMAT

Typical zone widths of a binary-optics aberration correction pattern can vary from several hundred microns to less than one micron. In the absence of a means to modulate the write beam spot size (by, for example, intentional defocusing), an efficient format was devised for writing zones of any size with a single-sized spot. The writing formats are shown in Fig. 6.

Since the quality and positional accuracy of the zone edges ultimately affects optical component performance, they are written with accurately positioned concentric and contiguous ring exposures.

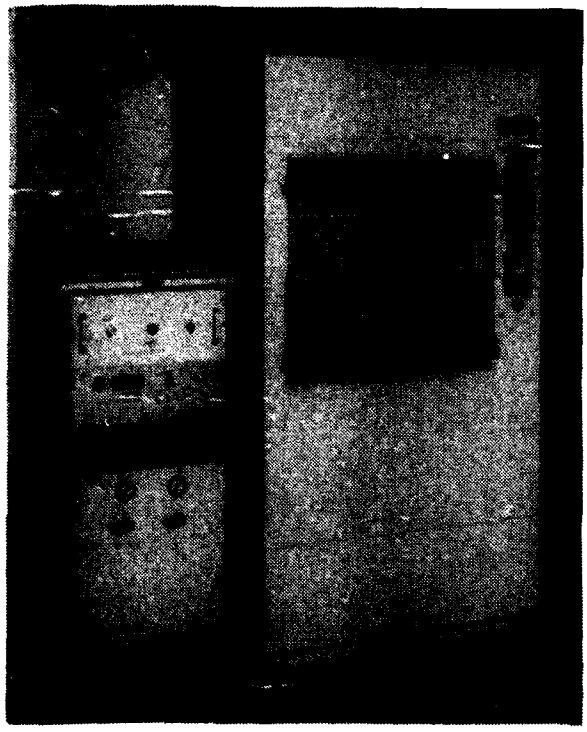

Figure 5: Photograph of the environmental chamber enclosing the laser writer mechanical and optical components. The instumentation rack on the left houses the pneumatic and electrical control units for the air-bearing slide and spindle.

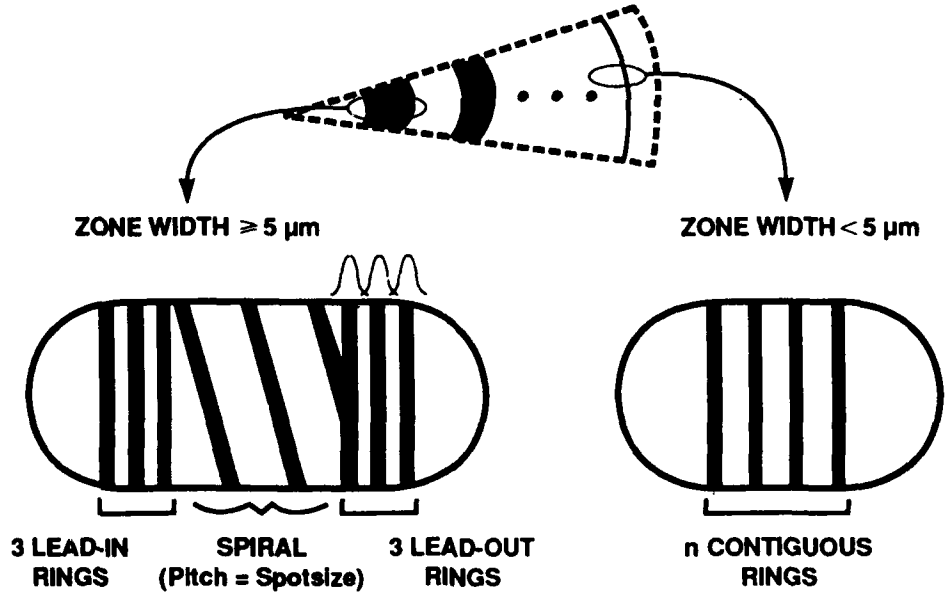

Figure 6: Illustration of the writing formats. For zones of width greater than 5 µm, a spiral pattern is written between boundary rings to reduce write time.

During this process, the write beam is intensity-modulated syncronously with spindle rotation to expose the photoresist for just one revolution of the spindle. Writing the boundary rings is a time consuming process because of the slide settling time, but exposing the photoresist between zone boundaries does not require high positional accuracy. Therefore, after writing the boundary rings, the beam is scanned between the rings in a constant velocity mode, forming a spiral pattern with spot-size pitch. While in the spiral mode, the beam is modulated syncronously with slide radial motion to eliminate the possibility of overexposure at the spiral ends. For improved zone

edge control it has been found empirically that three concentric rings on either edge of a zone are necessary, but this requirement is machine dependent. With this format, zones widths down to approximately 5 μm can be written.

For zone widths less than 5 μm the spiral mode is eliminated and the zone is written with an appropriate number of properly spaced concentric rings. In principle, zones widths down to the write-beam spot size ($\approx 0.7\ \mu m$) should be possible, but have yet to be reliably demonstrated.

Write time might be expected to depend only on the component aperture size for a constant spindle angular velocity and constant write-beam spot size. However, the writing formats above introduce a length of time required for accurately positioning the zone edges that is independent of zone width. This overhead time makes total write times dependent on the number of zones in a pattern as well as the pattern area.

4. DIRECT-WRITE LENS EXAMPLE

4.1. Design

To illustrate pattern writing accuracy, we have fabricate an F/10 two-phase-level lens by writing directly on a SiO_2 substrate. Pattern design and lens fabrication steps are outlined below.

The phase function for a fully corrected on-axis lens designed for collimating a point source can be expressed as

$$\phi(r) = \frac{2\pi}{\lambda}\left[\sqrt{f^2 + r^2} - f\right] \tag{1}$$

where f is the lens focal length, λ is the wavelength of incident light and r is the radial position from the optical axis. The diffractive lens surface profile is found by a two step process. First the phase function is evaluated modulo 2π and then a multilevel approximation of this new function is constructed. The binary optics approximation divides the function into 2^M quantized phase levels represented by M masks. In general, the quantized phase is

$$\phi(r) = \frac{2n\pi}{2^m} \tag{2}$$

where n is the phase transition index and m is the mask number, running from 1 to M. The phase transition locations are found by setting Eq. 1 equal to Eq. 2 and solving the expression for r,

$$r_n = \sqrt{\frac{n\lambda f}{2^{m-1}} + \left(\frac{n\lambda}{2^m}\right)^2} \tag{3}$$

When $m = 1$ in Eq. 3 the radial positions of the zone edges for a two-phase-level lens are defined. Any two consecutive integer values of n give the two radial boundaries of a single region of constant phase. The binary amplitude mask associated with this lens consists, for example, of a transparent zone from r_1 to r_2 and an opaque zone from r_2 to r_3. A continuous phase profile evaluated modulo 2π and its corresponding two-phase-level approximation are shown schematically in Fig. 7.

Figure 7: Schematic diagram showing a continuous phase profile evaluated modulo 2π and a two-phase-level approximation. r_n is the radial position of a phase level transition.

The number of zones in the total pattern for a lens can be found by solving Eq. 2 for n with $r = D/2$, where D is the optical element diameter, and dividing the result by 2 since there are two transitions for each zone. The pattern for our F/10, 50.8 mm diameter lens consists of ≈ 1000 zones, the smallest of which is 6.3 μm.

4.2. Fabrication

The binary optics fabrication process consists of three essential steps. The first step involves designing and fabricating a set of master amplitude masks which describe the desired surface relief profile. In the next step, the mask pattern is transferred to the photoresist-coated surface of the optical element by contact photolithography. Finally, the substrate surface is etched in those areas where the photoresist was not exposed. It is our main purpose here to describe the first step of this process–a method of mask fabrication using a polar-coordinate laser writer. However, by additional processing of a mask generated using this method, a two-phase-level lens can be made. Since the pattern for this lens is not transferred to the substrate by contact lithography, but is instead directly written onto the substrate, the optical element is referred to as a direct-write lens.

An amplitude mask is nothing more than a substrate that has had a uniform coating of a low-transmittance material selectively etched. Our laser writer masks employ an evaporation-deposited metal film for the low-transmittance material. After spin-coating the metal layer with photoresist, the desired pattern is recorded in the resist with the laser writer.

As the writing process entails coupling coherent monochromatic light into an etalon formed by the highly reflective metallic coating and high refractive index resist coating, the effect of standing wave patterns in the photoresist on line width control must be considered. Presently, our best solution is to control the metal and photoresist layer thicknesses precisely and then characterize the exposure parameters under these restricted conditions. The optimum exposure energy for this demonstration of 320 mJ/cm^2 was found empirically from a number of test runs with an Al film thickness of 800 Å and a Shipley 1400-17 resist thickness of 0.32 μm. The standing wave problem is particulary severe with our high reflectivity metal films as evidenced by the high energy required to fully expose the resist. The typical exposure energy given for this resist in the absence of a high reflectivity coating is 20 mJ/cm^2.

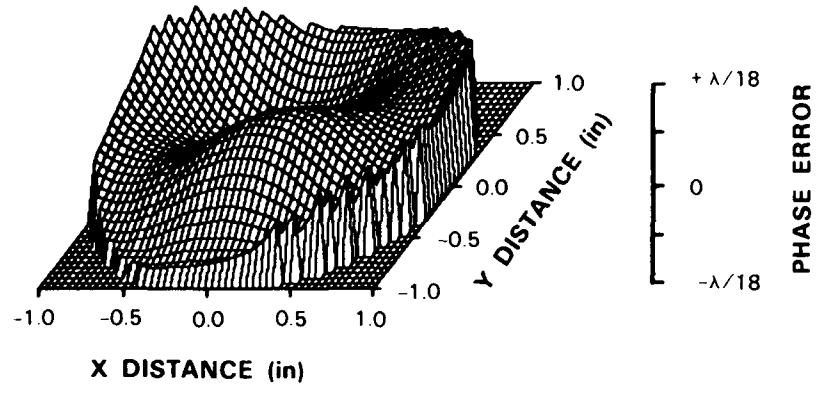

Figure 8: Wavefront quality of an F/10 binary optics lens. The wavefront error is $\lambda/40$ rms and $\lambda/9$ peak to valley.

To write our F/10 mask pattern, the expression for the zone-edge radial positions given by Eq. 3 was entered into the process control PC and a data file of zone-edge radii was stored on the PC hard disk. The lens pattern required less than 2 hours to write at a spindle speed of 1000 RPM. After exposure, the resist was developed in a 1:1 dilution of Microposit Concentrate Developer and deionized water for 28 seconds. The substrate was then oxygen-plasma ashed for 15 seconds to remove any residual photoresist from the clear pattern areas. Finally, the Al film was wet-etched to form the binary amplitude mask and the remaining photoresist was removed.

At this point a mask fabrication process would be complete. For our direct-write component, however, we continued by spinning on a 0.5 μm layer of photoresist and back-exposing it through the Al amplitude pattern using a Hg lamp. After developing the resist and plasma ashing, substrate material was selectively removed by reactive-ion etching in a CHF_3 plasma. The substrate was etched to a target depth of one-half-wave retardation, or 6989 Å in SiO_2 for an incident helium-neon laser wavelength of 6328 Å. The actual measured depth of 7520 Å represents a 7.6% error.

4.3. Optical performance

The first-diffraction-order wavefront error of this F/10 lens was measured with a Zygo interferometer and the results are displayed in Fig. 8. The rms error is $\lambda/40$, the peak-to-valley error is $\lambda/9$, and the predicted Strehl ratio is 0.98. Since the substrate was specified to be flat to $\lambda/10$, these results show the wavefront quality to be essentially substrate-limited.

First order diffraction efficiency was measured to be 38.6%. After accounting for the 0.6% error attributed to etch-depth overshoot, this result is only 1.3% below the theoretical efficiency of 40.5%. Zone-edge quality of the 6.3 μm features is very good, as can be seen in the x625 optical microscope picture in Fig. 9. These results indicate that the lens pattern generated by our laser writer is quite precise.

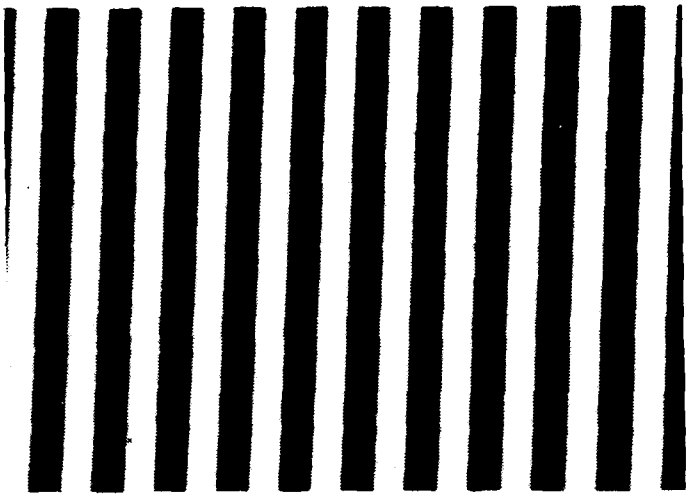

Figure 9: View of F/10 lens smallest features (line width is 6.3 μm) through a x625 optical microscope.

5. CONCLUSIONS

We have successfully shown by experiment the viability of a polar-coordinate laser writer. Specifically, we have demonstrated an alternative to E-beam mask fabrication that meets all of our initial design goals; this machine was developed in a very short time, with a minimum of effort and expense,and total mask fabrication times have been reduced to hours rather than days as normally required by an E-beam mask foundry. The measured performance of an F/10 lens written with this machine shows that savings in time and expense have not resulted in a sacrifice in quality.

This work represents the early accomplishments of an ongoing development effort. Some goals for the future are: (1) developing the capability to reliably write zones of less than 1 μm width, (2) writing on curved substrates; (3) writing multi-level patterns either by tailoring the photoresist profile during a single write process or by successive registration of the substrate on the spindle, and (4) writing modulo 2π continuous phase profiles.

6. ACKNOWLEDGEMENTS

This work has benefitted from the numerous contributions of Gary Swanson, the binary optics fabrication expertise of William Delaney and the generous support and guidance of Wilfred Veldkamp. We also acknowledge Trent DePersia of DARPA for sponsoring this project.

The views expressed are those of the authors and do not reflect the official policy or position of the U.S. Government.

7. REFERENCES

1. J.R. Leger, and M. P. Griswold,"Binary optics miniature Talbot cavities for laser beam addition," Appl. Phys. Lett. **56**, No. 1, 4-6 (1990).

2. G. J. Swanson, and W. B. Veldkamp,"Diffractive optical elements for use in infrared systems," Op. Eng. **28**, No. 6, 605-608 (1989).

3. W. Goltsos, and M. Holz,"Binary micro optics: an application to beam steering," SPIE **1052**, 131-141 (1989).

4. L. Lesem, P. Hirsch, and J. Jordan,"The kinoform: a new wavefront reconstruction device," IBM J. Res. Dev. **13**, 150 (1969).

5. V. M. Vedernikov, V. N. Vyukhin, V. P. V. P. Koronkevich, F. I. Kokoulin, A. I. Lokhmatov, V. I. Nalivaiko, A. G. Poleshchuk, G. A. Tarasov, V. A. Khanov, A. M. Shcherbachenko, and Yu. I. Yurlov,"A precision photoconstructor for synthesizing optical components," Autometriya **3**, 3 (1981) (in Russian, Engl. transl. Autom. monit. meas.).

6. V. P. Koronkevich, V. P. Viriyanov, F. I. Kokoulin, I. G. Palchikova, A. G. Poleshchuk, A. G. Sedukhin, E. G. Churin, A. M. Shcherbachenko, and Yu. I. Yurlov,"Fabrication of kinoform optical elements," Optik **67**, No. 3, 257-266 (1984).

7. T. Yatagai,J. G. Camacho-Basilio, and H. Onda,"Recording of computer-generated holograms on an optical disk master," SPIE **1052**, 119-124 (1989).

8. See, for example, D. K. Cohen,W. H. Gee, M. Ludeke, and J. Lewkowicz,"Automatic focus control: the astigmatic lens approach," Appl. Opt. **24**, 565-570 (1984).

9. F. Jones,"The Refractivity of Air," J. Res. Natl. Bur. Stand. **86**, 27-32 (1981).